Acta of Bioengineering and Biomechanics
Vol. 23, No. 1, 2021

Original paper
DOI: 10.37190/ABB-01757-2020-05

Effect of polyethylene glycol on surface coating of Ta_2O_5 onto titanium substrate in sol-gel technique

VAMSI KRISHNA DOMMETI, SUMIT PRAMANIK*, SANDIPAN ROY*

Department of Mechanical Engineering, College of Engineering and Technology,
Faculty of Engineering and Technology, SRM Institute of Science and Technology,
Kattankulathur–603203, Kanchipuram, Chennai, TN, India.

Purpose: Recently, titanium (Ti) and its alloys have been widely used in dental and surgical implants in the last few decades. However, there is a loosening effect over a long period usage. Therefore, the present study aimed to increase life of an implant by its surface modification. *Methods*: In present study, sol-gel process has been applied to create tantalum pentoxide (Ta_2O_5) layer coating on Ti-substrate. In this technique, polyethylene glycol (PEG) plays an important role to form uniform porous coating, which can have potential application in formation of strong bonding to the natural bone. *Results*: Microstructural, elemental, structural and binding energy results showed that the material with 100% PEG-enhanced sol-gel Ta_2O_5 with spin coating onto Ti substrate followed by an optimized sintering temperature (500 °C) has better porous structure than that of 5% PEG-enhanced sol-gel Ta_2O_5 coating, and would be suitable for tissue in-growth properties. *Conclusions*: Therefore, it was concluded that the present spin coated 100% PEG-enhanced Ta_2O_5 coating onto Ti, having the most suitable morphology with enhanced roughness, could be noteworthy for potential tissue in-growth and it could provide desired bonding at the interface of Ti-implant coating and host tissues in biomedical applications.

Key words: *porous, coating, sol-gel, sintering, PEG, tantalum pentoxide*

1. Introduction

Metallic biomaterials, especially titanium (Ti) alloys, have been used in the different orthopaedic applications, including dental implants, because of their excellent chemical composition and surface morphology, which are most important parameters for enhancing the bone integration [28]. Further, oxide layers formed on implant material had shown some promising results for high corrosion resistance [10] and biocompatibility on titanium surface [4], [14], [28]. Among ceramics, hydroxyapatite (HA) has widely been used as a bioceramic coating material [2], [5], [12]. To deposit different apatite films such as HA or fluorapatite (FA) on Ti based substrate, sol-gel technique has shown good potential [12]. The biological performance of their uniform films in terms of their dissolution behavior and *in vitro* cell responses was evaluated as good one. However, the coating layers of pure apatite phase were mostly dense, which might not be suitable to form strong bonding with host tissues [12]. In this context, sol-gel technique had been used as easiest way to coat the glass-ceramic on to the Ti alloy (Ti_6Al_4V) substrate. The mechanical and biological performances of the coated Ti alloy were also found as good [24]. In another study, composition and cytocompatibility of the coating were compared between sol-gel and conventional plasma-sprayed HA coating specimens [9]. The inexpensive sol-gel-processed coating layer had shown no cracks and increased adhesion compared to conventional plasma–sprayed HA coat-

* Corresponding authors: Sumit Pramanik and Sandipan Roy, Department of Mechanical Engineering, SRM Institute of Science and Technology, Chennai-603203, India. E-mails: sumitprs@srmist.edu.in; sandipan888roy@gmail.com (SR), sandipag@srmist.edu.in (SR).

Received: November 21st, 2020
Accepted for publication: February 19th, 2021

ing [26]. It had been reported that a little amount of tantalum (Ta) along with HA in a HA/Ta composite film prepared by physical vapour deposition (PVD) had outstanding biocompatibility and improved corrosion resistance [23]. Interestingly, thin tantalum oxide hybrid coating layers obtained by sol-gel deposition showed improved bio-corrosion resistance in the body fluid, biocompatibility, and offered several multifunctionalities [5]. It accelerates the formation of bone-like apatite in simulated body fluid (SBF) [18]. In this context, β-tantalum pentoxide (β-Ta_2O_5) coating plays an important role in protection of orthopedic implants by enhancing its biocompatibility, bioactivity and corrosion resistance [34]. Generally, Ta_2O_5 ceramic has shown very high dielectric and good optical properties [7]. Recently, tantalum oxide coatings have been applied onto different metallic implant materials such as, Ti and its alloys [16], [17], [27], cobalt–chromium (Co–Cr) alloys [3], magnesium (Mg) alloys [8] in order to improve their corrosion, wear resistance and cell growth properties in human body.

After thorough reviewing of many related research studies, it has been noticed that sol-gel is a cheapest and most facile method [19], [30], [36]. In addition, morphology and chemical structures also could be responsible in order to obtain desired bonding and bioactivity properties of a coating [30]. However, some of these characteristics of Ta_2O_5 coating need to be improved as well as analysed more precisely. Therefore, this present research work aimed to develop polyethylene glycol (PEG)-enhanced sol-gel-processed thin layer coating of Ta_2O_5-based ceramics with porous microstructure. These coatings were applied using spin coating onto Ti substrate followed by an optimized sintering temperature (500 °C). Here, PEG was selected since it has been found as potential agent for making porous structure [20], [35]. The Ta_2O_5-based ceramics could be formed from many other conventional ways but one of the main objectives of this study is the formation a strong thinfilm coating of Ti_2O_5 on Ti-substrate. In ordered to do this, as per best of our knowledge, we found that sol-gel technique is the cheapest and the most efficient route of making coating without making an end product of complex compound, which might be toxic in nature. In addition, the main advantages of this method are most facile, ease, and inexpensive compared to the already used sol-gel techniques using tantalum alkoxides. Most importantly, this investigation also aimed to precisely analyze the morphological, chemical, structural surface characteristics and binding energy properties of Ta_2O_5 coatings.

2. Materials and method

2.1. Sol-gel process

The sol-gel Ta_2O_5 film has been produced by various researchers [19], [30], [33], [36]. In this study,

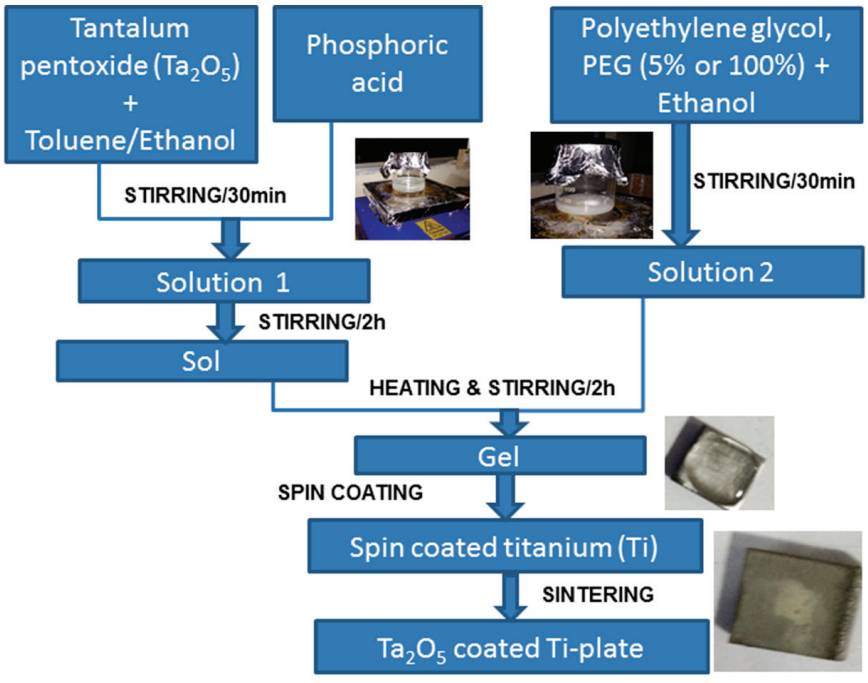

Fig. 1. Schematic of coating by sol-gel process

first, 0.022 g of tantalum pentoxide (Alfa Aesar, 99%) and 50 ml toluene/ethanol were taken in 1:1 (v/v) ratio [2]. Ta_2O_5 was mixed in 50 ml of toluene/ethanol solution and stirred vigorously for 30 min at constant 1000 rpm on magnetic hot plate to get a sol. Then, 15 ml of phosphoric acid (30% H_3PO_4) and two different amounts, such as 0.0456 g and 0.912 g (i.e., 100% PEG) of polyethylene glycol (PEG, MW400) were added and kept stirring vigorously for 2 h to obtain a gel (i.e., a thick transparent sticky solution). Here, the nomenclature of 100% PEG indicates the maximum amount (0.912 g) of PEG used in the 15 ml H_3PO_4 solution to form the gel whereas 0.0456 g or 5% (w/w) of used maximum PEG in same amount of H_3PO_4 solution. It is necessary to inform that other acid could also have been used, but main advantages of H_3PO_4 used in this study are having excess phosphate group that may help form strong bond between the coating and Ti-substrate, and, most importantly, being non-toxic [21]. The H_3PO_4 also has ability to modify the surface of oxide ceramic, i.e., Ti_2O_5, in order to make strong bond with the substrate [6]. The entire sol-gel process is depicted in Fig. 1.

The same method was followed to obtain both the sol-gel solutions only just by varying amount of PEG of 0.0456 g (i.e., 5% PEG) and 0.912 g (i.e., 100% PEG) in gel 1 and gel 2, respectively, in order to check the effect of PEG on pore formation. Here, PEG plays a vital role in formation of proper pore size and porosity being evaporation during sintering [20]. There are different kinds of sol-gel method, but in the present study, xerogel process was used since high shrinkage was needed to get the thin film. Indeed, there was formation of alkoxide of tantalum in fresh gel, which was turned back into Ta_2O_5 after sintering process.

2.2. Titanium subtract preparation

Commercial titanium plates (Ti-plates) of grade 5 ($10 \times 10 \times 2$ mm^3) were used for substrate. Ti-plates were polished by using emery papers of different grades (400, 600, and 1200). The main purpose of polishing with emery sheet was to achieve proper adhesion and uniform dispersion of sol-gel onto the surface of the Ti-substrate.

2.3. Spin coating

The polished substrates were preheated up to 50 °C and the PEG-enhanced sol-gel-processed Ta_2O_5 was coated on the polished Ti-substrates at 3000 rpm speed for 20 s, using a home-made spin coater, in which spin was controlled by TCRT5000 infrared (IR) sensor [5]. It is necessary to inform that microbubbles formation was controlled by tuning the spinning speed. It was observed that the formation of micro-bubble was minimum and the porous coating onto the Ti-substrate was more uniform for the gel 2 compared to gel 1.

2.4. Sintering steps

After coating, the sol-gel-processed Ta_2O_5-coated Ti-substrate specimens were sintered up to 500 °C [31]. Sintering was performed very slowly with a three-step sintering technique using PID controller in a programmable muffle furnace. In the first step, the samples were heated up to 100 °C for 1 h; in the second step, the temperature was raised to 350 °C and held for 2 h; in the third step, the temperature was again raised to 500 °C and isothermal soaking for 75 min followed by furnace cooling for getting fine crack-free crystallization [25].

2.5. Characterizations

After sintering, sol-gel-processed Ta_2O_5-coated Ti-substrate specimens were analyzed precisely with different characterizations techniques. The crystal structure of coated specimens was studied by x-ray diffraction (XRD) technique with CuKα radiation using x-ray diffractometer (XPert Pro, PANalytical) in the 2θ range of 10°–90°. Microstructures of the sintered specimens were analyzed using inverted metallurgical microscope (BX-KMA-LED, Olympus) and field emission scanning electron microscope (FESEM, Quanta 200, FEI). The FESEM images were captured in the secondary electron mode. The coating thickness was also computed from FESEM images. The energy dispersive spectroscopy (EDS) with in-built FESEM machine was used to inspect the presence of several elements used in sol-gel process. Fourier transformed infrared spectra of the coated specimens were recorded at a wavenumber range of 400–4000 cm^{-1} using Fourier transformed infrared (FTIR) spectroscope (IRTRACER 100, SHIMADZU). Both spectroscopic analyses were used to check for the presence of functional groups and their interaction in the coated surfaces. X-ray photoelectron spectroscopy was employed to identify the chemical constituents and elemental states of the different coated Ti samples very precisely using X-ray photoelectron spectroscope (XPS, PHI5000 Version Probe III, ULVAC-PHI, Inc) with travel range and drive axis of ± 400 μm and 500 nm, respectively, in

x-axis. The binding energies were calibrated for titanium, tantalum, phosphorus, oxygen, and carbon.

3. Results

3.1. XRD study

X-ray diffraction patterns of pure titanium substrate, gel 1-coated Ti, gel 2-coated Ti, sintered gel 1-coated Ti, and sintered gel 2-coated Ti are depicted in Figs. 2a–e, respectively. The crystallite size of different phases (viz., Ti, Ta_2O_5, and TiP_2O_7) and the peak intensity ratios for (001) Ta_2O_5 to (002) Ti and (630) TiP_2O_7 to (002) Ti of XRD samples are illustrated in Table 1. The average crystallite size was calculated from the half width full maxima, FWMH (included instrumental broadening) of the all peaks for the individual phases using Debye–Scherer relation, while the $[I_{Ta_2O_5(001)}/I_{Ti(002)}]$ ratio was used for the unsintered samples for both the gel coated samples since they don't have the (630) peak of TiP_2O_7 [20]. Hereby, shape factor K of 0.89 was considered as a most widely used constant value. It is noteworthy that since unsintered coatings were amporphous in nature, compared to the sintered peaks, the (001) peak of Ta_2O_5 seems appeared as lower intense and thus negligible in the present comparison graph-scale. However, in individual plot obtained by precise analysis, this (001) peak of Ta_2O_5 is also found as broad peak in unsintered condition with intensity around 4900 Cts for sample b and but small sharp peak having intensity around 5500 Cts with slight shifting to $2\theta \sim 21.85°$ from standard position for the sample c shown in Fig. 2. This small peak intensity difference happened since sample b is formed as a thinner coating compared to the sample c in Fig. 2.

3.2. Microstructure analysis

Morphological analyses were carried out by optical microscope as well as FESEM. Optical and FESEM microstructures of pure titanium substrate, sintered gel 1-coated Ti, and sintered gel 2-coated Ti are depicted in Figs. 3 and 4, respectively. The elemental analysis recorded by EDS study for both the sintered coated Ti specimens and uncoated Ti substrate is depicted in Fig. 5. In Figure 6, the actual thickness of both the coatings for sintered coated Ti specimens is depicted.

Table 1. Crystallite size of different phases and the peak intensity ratio of XRD samples

Phases	Unit	Crystallite size or Peak intensity ratio of the samples				
		a	b	c	d	e
Ta_2O_5	nm	na	139.05	213.22	163.73	241.11
TiP_2O_7	nm	na	–	–	163.34	122.89
Ti	nm	136.04	141.24	159.34	188.07	179.80
XRD peak intensity ratio						
$[I_{Ta_2O_5(001)}/I_{Ti(002)}] \times 100$	%	na	25.31	26.13	105.58	287.64
$[I_{TiP_2O_7(630)}/I_{Ti(002)}] \times 100$	%	na	–	–	86.58	218.83

Note: (a) pure titanium (α-Ti) substrate, (b) gel 1-coated Ti, (c) gel 2-coated Ti, (d) sintered gel 1-coated Ti, and (e) sintered gel 2-coated Ti.

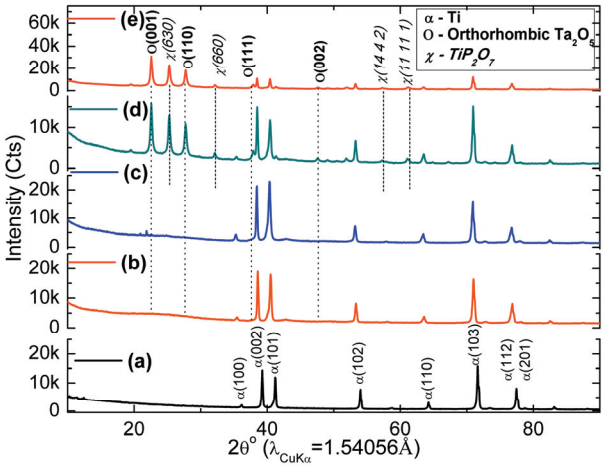

Fig. 2. X-ray diffraction patterns of (a) pure titanium (α-Ti) substrate, (b) gel 1-coated Ti, (c) gel 2-coated Ti, (d) sintered gel 1-coated Ti, and (e) sintered gel 2-coated Ti, (Hexagonal Ti: JCPDS No. 00-005-0682, Orthorhombic Ta_2O_5: JCPDS No. 00-001-0455, Cubic TiP_2O_7: JCPDS No. 00-038-1468)

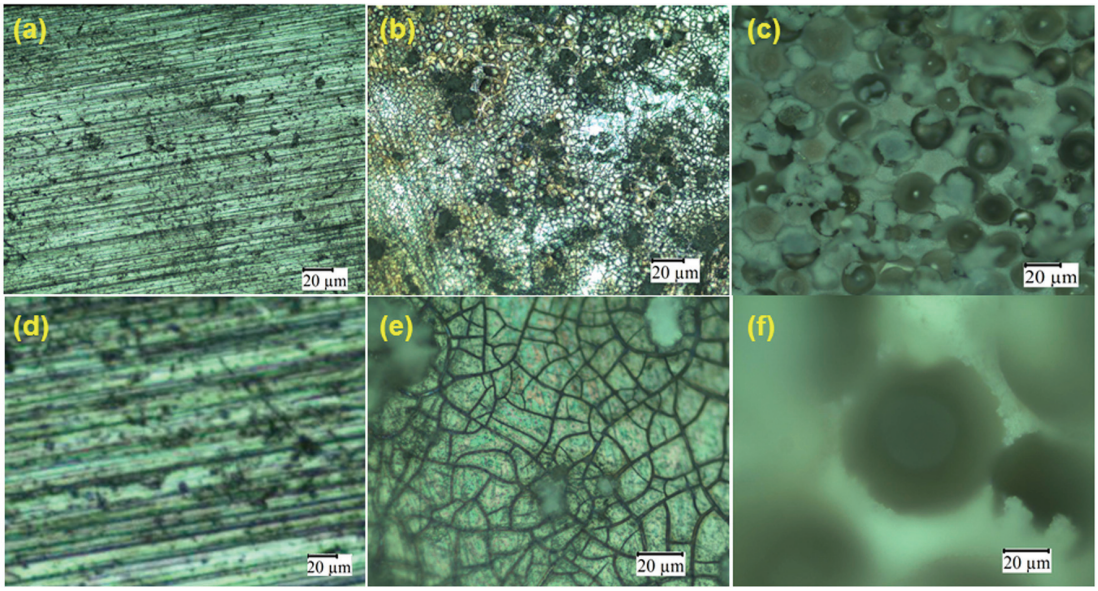

Fig. 3. Optical micrographs of (a, d) pure titanium (α-Ti) substrate,
(b, e) sintered gel 1-coated Ti, and (c, f) sintered gel 2-coated Ti

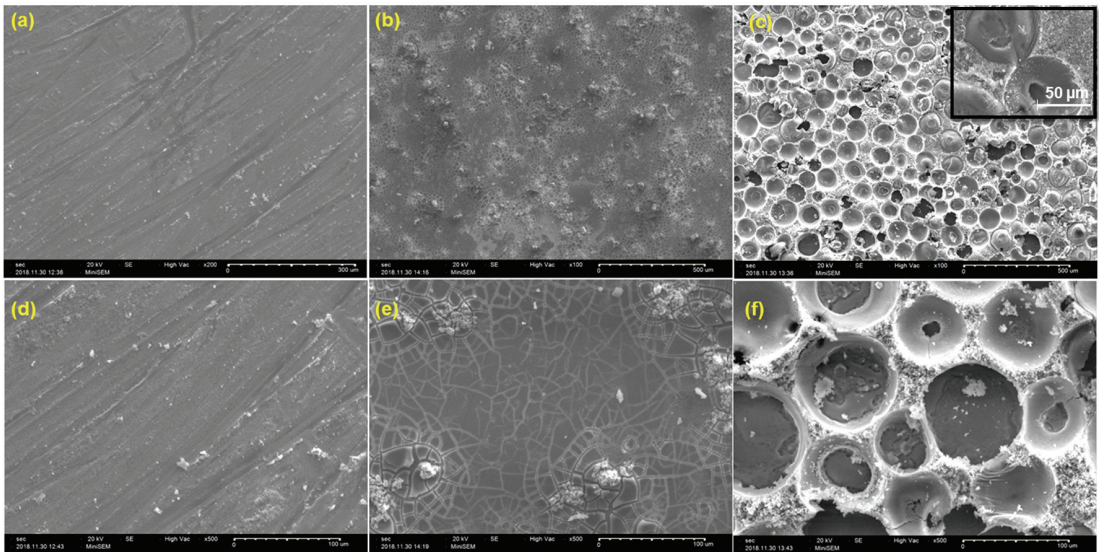

Fig. 4. FESEM micrographs of (a, d) pure titanium (α-Ti) substrate,
(b, e) sintered gel 1-coated Ti, and (c, f) sintered gel 2-coated Ti

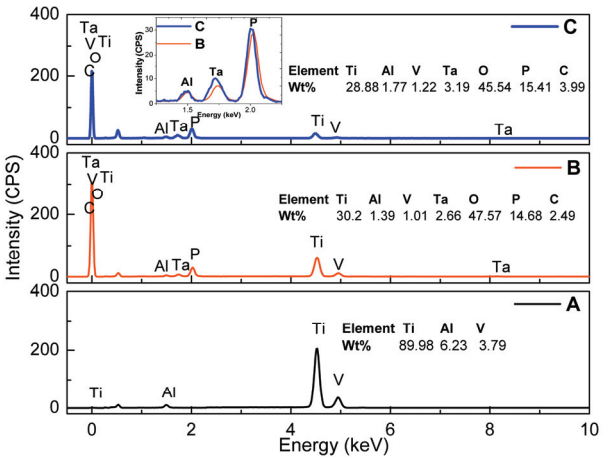

Fig. 5. EDS spectra of (A) pure titanium (α-Ti) substrate,
(B) sintered gel 1-coated Ti, and (C) sintered gel 2-coated Ti

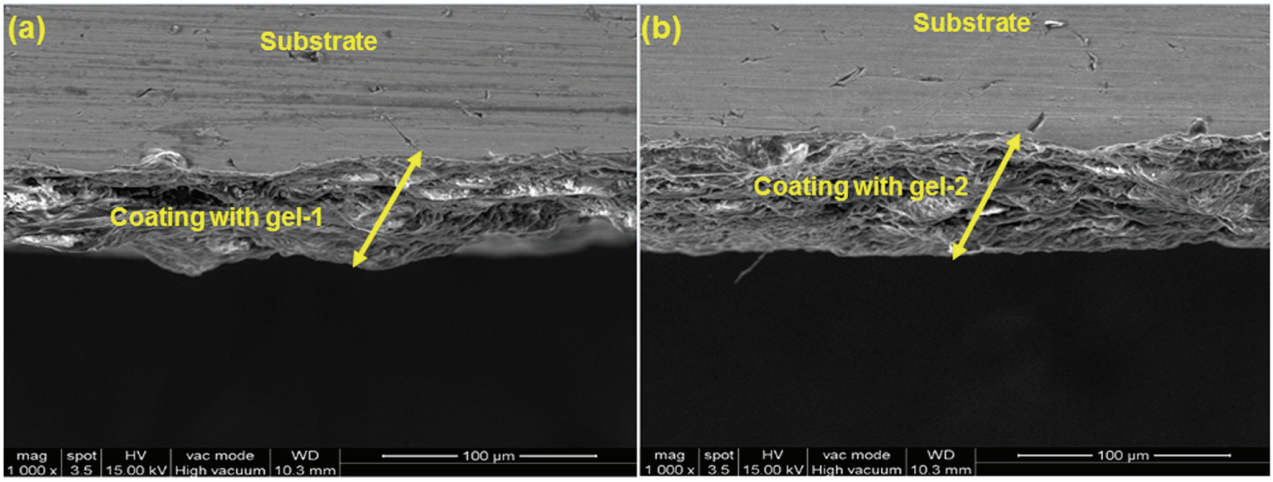

Fig. 6. FESEM micrographs of cross-sectional thickness of (A) sintered gel 1-coated Ti and (B) sintered gel 2-coated Ti specimens

3.5. FTIR spectroscopy

Figure 7 represents the FTIR spectra of pure titanium substrate, sintered gel 1-coated Ti, and sintered gel 2-coated Ti.

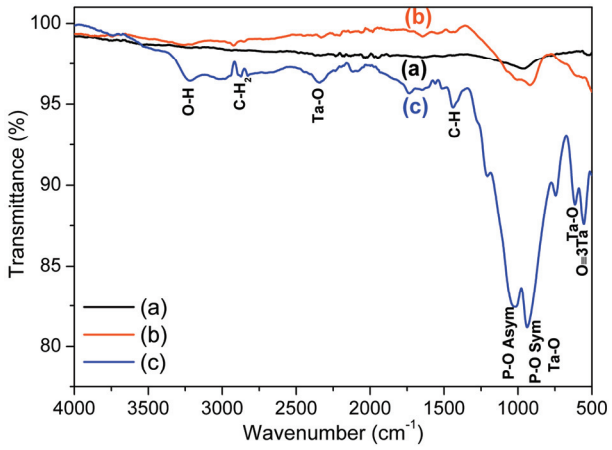

Fig. 7. FTIR spectra of (a) pure titanium (α-Ti) substrate, (b) sintered gel 1-coated Ti, and (c) sintered gel 2-coated Ti

3.6. Surface roughness measurement

The surface roughness parameters of titanium substrate, sintered gel 1-coated Ti, and sintered gel 2-coated Ti are illustrated in Table 2. Figure 8 represents the surface roughness behaviour of the coating.

Table 2. Surface roughness parameters of titanium substrate, sintered gel 1-coated Ti, and sintered gel 2-coated Ti

Sample	R_a [µm]	R_z [µm]
Ti-substrate	0.1126	0.8415
Sintered gel 1-coated Ti specimen	2.84	19.6662
Sintered gel 2-coated Ti specimen	3.79	18.5173

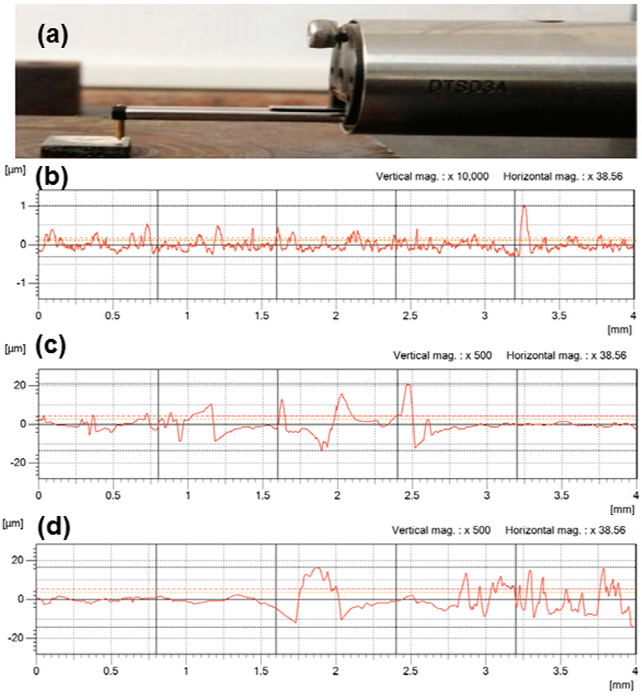

Fig. 8. (a) Surface roughness meter and surface roughness plots of (b) pure titanium (α-Ti) substrate, (c) sintered gel 1-coated Ti, and (d) sintered gel 2-coated Ti

3.7. XPS analysis

XPS spectra of the sintered gel 1-coated Ti and sintered gel 2-coated Ti specimens are shown in Fig. 9.

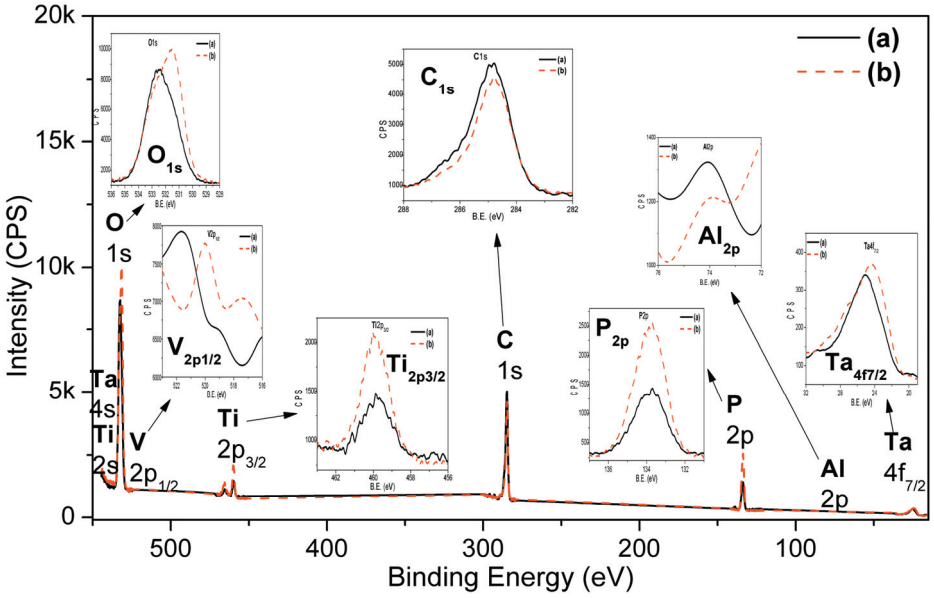

Fig. 9. XPS spectra of (a) sintered gel 1-coated Ti and (b) sintered gel 2-coated Ti

Table 3. Binding energy (BE) and atomic percentage of the elements present at the coated surface of sintered gel 1-coated Ti and sintered gel 2-coated Ti specimens

Elements	Sintered gel 1-coated Ti (Thin)			Sintered gel 2-coated Ti (Thick)		
	BE [eV]	Source	At%	BE [eV]	Source	At%
Ta $4f_{7/2}$	25.08	Ta_2O_5	0.3	24.22	Ta_2O_5	0.4
Ta4s	548.38			550.22		
Al_{2p}	74.04	Substrate	*	73.89	Substrate	0.2
P_{2p}	133.73	Pyrophosphate	5.5	133.73	Pyrophosphate	11.4
C_{1s}	284.78	C-C of PEG	39.3	284.78	C-C of PEG	31.2
$Ti2p_{3/2}$	554.78	Substrate	0.8	553.65	Substrate	3.0
Ti2s	559.88			460.03		
$V2p_{1/2}$	521.60	Substrate	*	520.00	Substrate	0.1
O1s	532.38	Ta_2O_5	54.1	531.53	Ta_2O_5	53.7

* Untraceable.

4. Discussion

4.1. XRD study

Based on Figure 2, it has been found that XRD peaks of the raw titanium substrate resembled α-Ti phase of hexagonal crystal structure (JCPDS No. 00-005-0682). After gel coating, the small amorphous peaks of orthorhombic crystal structure of Ta_2O_5 (JCPDS No. 00-001--0455) appeared [1]. After sintering, the Ta_2O_5 peaks became more crystalline as well as sharp intense peaks were found in XRD patterns [22]. Since more intense peaks of the Ta_2O_5 were found for 100% PEG, i.e., for gel 2-coated Ti, it clearly indicates that the thickness of this coating was produced during sol-gel process, compared to 5% PEG, i.e., for gel 1-coated Ti. It indicates that more amount of PEG content gel has higher ability to carry more amount of Ta_2O_5 as 100% PEG gel has shown higher thickness, compared to the 5% PEG gel. This result was later confirmed by morphological studies. It is to be mentioned that some amount of new phase of titanium pyrophosphate (TiP_2O_7) of cubic crystal (JCPDS No. 00-038-1468) was also produced

after sintering because of the reaction of metallic titanium with phosphoric acid. This extra peak of TiP_2O_7 was distinctly found in XRD patterns. Furthermore, as per XRD study, the (001) and (110) peaks of Ta_2O_5 have shown significantly higher intensity as well as greater total peak area, compared to the (630) of TiP_2O_7. So, the main product of this present study is Ta_2O_5 along with some side product TiP_2O_7, which is not toxic since it has pyrophosphate group. The crystallite size illustrated in Table 1 increased after sintering for both coated samples and it has increased significantly for the 100% PEG gel-coated samples, compared to the 5% PEG samples. Interestingly, the signature XRD peak ratio of coating ceramic to titanium substrate increased for the 100% PEG gel-coated samples, compared to the 5% PEG samples. This result indicates that the sintered 100% PEG gel-coated material has higher crystallinity compared to 5% PEG gel coating.

4.2. Microstructure analysis

Both optical and FESEM microstructures shown in Figs. 3 and 4 revealed that the coating morphology on sintered gel 2-coated Ti specimens was thicker and had more uniformly distributed desired sized pores of average 175 μm (70–300 μm) than that of gel 1 coated samples. It needs to be mentioned that the pore sizes between 100 μm and 500 μm are favourable for bone osteoclast formation [29]. In contrast, the coating morphology on sintered gel 1-coated Ti specimens showed entirely cracked surface. Therefore, gel 2 coating is considered better than gel 1 coating in the present study. The EDS results shown in Fig. 5 indicate that more amount of Ta_2O_5 is present in the sintered gel 2-coated Ti specimens than the sintered gel 1-coated Ti specimens. In the inset image of Fig. 5, it has been noticed that the Ta content (at around 1.72 keV) is significantly higher in gel 2 coating than that of the gel 1 coating. Since there is higher amount of total oxygen content in both the Ta_2O_5 and TiP_2O_7, the overall weight percentage of tantalum might be reduced compared to other studies owing to the side product (i.e., TiP_2O_7) [2], [5]. The thickness of the coatings was also measured as 45–61 μm and 58–72 μm for sintered gel 1-coated Ti and sintered gel 2-coated Ti specimens, respectively from the Fig. 6.

4.5. FTIR spectroscopy

In Figure 7, it can be seen that the metallic Ti substrate didn't show any significant IR peaks but other two samples showed some significant IR peaks, which are attributed to coating materials. The peaks at wavelenghts of 550 and 615 cm^{-1} can be attributed to the O≡3Ta or Ta–O–Ta stretching vibrations [15], and the peak at 2340 cm^{-1} may be attributed to Ta–O vibration mode [1]. The peaks at around 930 and 1025 cm^{-1} corresponded to P–O of pyrophosphate $(P_2O_7)^{4-}$ from titanium pyrophosphate ($Ti_2P_2O_7$) [9]. The new $Ti_2P_2O_7$ phase formation was also supported by our XRD results. The peak at 930 cm^{-1} also matched with Ta–O–Ta bonding. Few peaks of PEG remaining also revealed at around 1440, 2889 and 3240 cm^{-1}, which correspond to C-H bonding of alkane, symmetric $–C–H_2$ stretching and alcoholic OH bonds, respectively [19]. Since the use of more PEG resulted in formation of more crystalline porous Ta_2O_5 growth onto the Ti substrate, the FTIR spectrum of sintered gel 1-coated Ti specimen showed more intense transmittance peaks compared to the other specimens. The chemical analysis also strongly supports our other results.

4.6. Surface roughness measurement

It can be seen from Fig. 8 that the average surface roughness (R_a) also known as surface profile is one of most important parameters of surface topology. R_a is statistically a very stable, repeatable parameter and it is good for random type surfaces, such as grinding [25], [32]. Another important is parameter is denoted as R_z, which is mean peak-to-valley height and important for porous surfaces. These important roughness parameters are illustrated in Table 3. Both parameters indicate that the substrate surface of Ti-plate became significantly smoother after coating while sintered gel 2-coated Ti specimen showed highest R_a value but slightly lower R_z value compared to sintered gel 1-coated Ti specimen. The later result was what might be the cause of crack formation. After crack formation in some place, the layer detached from the substrate of the surface and R_z value was higher in sintered gel 1-coated Ti specimen compared to other specimens. It was also evidently observed in the micrographs in Figs. 3e and 4e.

4.7. XPS analysis

The XPS results shown in Fig. 9 represent the surface chemistry of the two coated specimens. The binding energy shifting of the elements present at the

coating surface indicates the precise amount of their chemical bonding, as illustrated in Table 3. The related XPS peaks also were in accordance with other study [13]. It clearly indicates that shifting of binding energy (BE) of the present elements happened because of the effect of PEG, which might be left as residual chemisorbed carbon even after sintering. It needs also to be stated that excess amount of carbon present in the gel 1-coated Ti might be owing to the dual effect of atmospheric carbon as well as absence of Al_{2p} as well as $V2p_{1/2}$ in the thin coating. Since the film was very thin for gel 1-coated Ti compared to gel 2-coated Ti, it was more prone to get attack by atmosphere [13]. On the other hand, since the coating film of the gel 2-coated Ti was more porous than that of gel 1, all the possible peaks of substrate materials, including Al_{2p} as well as $V2p_{1/2}$ were detected properly in XPS.

5. Conclusions

In the present study, coating of thin Ta_2O_5 layer was produced on the Ti-substrate using sol-gel method. The role of PEG in the formation of uniform porous coating has been investigated. The uniformly porous microstructure (300 μm) with presence of desired elements indicates that the 100% PEG-enhanced sintered sol-gel Ta_2O_5 with spin coating onto Ti substrate providess attractive and suitable surface for tissue ingrowth [11], [19]. The amount of Ta^{5+} increased with higher amount of PEG, which can enhance the cell growth. Thus, the sol-gel-processed Ta_2O_5 coating may have potential applications in formation of strong bonding to the natural bone, as reported in other studies. Hence, it can be concluded that the present spin-coated Ta_2O_5 onto Ti, having most suitable morphology with suitable roughness, may be suitable for tissue-implant material interaction by facilitating desired bonding at the interface of Ti-implant coating and host tissues in dental or orthopedic applications. Therefore, this study predicts the suitable porous coating on the dental implants for facilitating the host tissue-growth, which might be confirmed by cell culture study in future.

Acknowledgements

Authors acknowledge Metallography Laboratory and Foundry Laboratory, Department of Mechanical Engineering and Nanotechnology Research Centre, SRM Institute of Science and Technology for accessing their research facilities like syntheses and XRD, XPS as well as FTIR, respectively.

References

[1] ARBUJ S.S., MULIK U.P., AMALNERKAR D.P., *Synthesis of Ta_2O_5/TiO_2 coupled semiconductor oxide nanocomposites with high photocatalytic activity*, Nanosci. Nanotechnol. Lett., 2013, 5, 968–973.

[2] ARNOULD C., VOLCKE C., LAMARQUE C., *Titanium modified with layer-by-layer sol–gel tantalum oxide and an organodiphosphonic acid: A coating for hydroxyapatite growth*, J. Colloid Interface Sci., 2009, 336, 497–503.

[3] BALAGNA C., FAGA M.G., SPRIANO S., *Tribological behavior of a Ta-based coating on a Co–Cr–Mo alloy*, Surf. Coat Technol., 2014, 258, 1159–1170.

[4] CHANG Y.Y., HUANG H.L., CHEN H.J., LAI C.H., WEN C.Y., *Antibacterial properties and cytocompatibility of tantalum oxide coatings*, Surf. Coat Tech., 2014, 259, 193–198.

[5] FATHI M., AZAM F., *Novel hydroxyapatite/tantalum surface coating for metallic dental implant*, Mater. Lett., 2007, 61, 1238–1241.

[6] FRANCISCO M., CARDOSO W., GUSHIKEM Y., *Surface modification with phosphoric acid of SiO_2/Nb_2O_5 prepared by the Sol-Gel method: structural−textural and acid sites studies and an ion exchange model*, Langmuir, 2004, 20, 8707–8714.

[7] GEORGIEV R., GEORGIEVA B., LAZAROVA K., VASILEVA M., BABEVA T., *Sol–gel tantalum pentoxide thin films with tunable refractive index for optical sensing applications*, Opt. Quantum Electron., 2020, 52 (10), 1–12.

[8] GUL C., ALBAYRAK S., CINICI H., *Characterization of Tantalum Oxide Sol–Gel-coated AZ91 Mg Alloys*, Trans. Indian Inst. Met., 2020, 73 (5), 1249–1256.

[9] GUPTA S.K., MOHAPATRA M., GODBOLE S., *On the unusual photoluminescence of Eu^{3+} in α-$Zn_2P_2O_7$: a time resolved emission spectrometric and Judd–O felt study*, RSC Adv., 2013, 3, 20046–20053.

[10] HEE A.C., JAMALI S.S., BENDAVID A., MARTIN P.J., KONG C., ZHAO Y., *Corrosion behaviour and adhesion properties of sputtered tantalum coating on Ti_6Al_4V substrate*, Surf. Coat Tech., 2016, 307, 666–675.

[11] INNOCENTINI M., FALEIROS R., PISANI R., *Permeability of porous gelcast scaffolds for bone tissue engineering*, J. Porous Mater., 2010, 17, 615–627.

[12] KIM H.-W., KIM H.-E., KNOWLES J.C., *Fluor-hydroxyapatite sol–gel coating on titanium substrate for hard tissue implants*, Biomaterials, 2004, 25, 3351–3358.

[13] KŁONICA M., KUCZMASZEWSKI J., *Modification of Ti_6Al_4V Titanium Alloy Surface Layer in the Ozone Atmosphere*, Mater. Des., 2019, 12, 2113.

[14] KOKUBO T., *Design of bioactive bone substitutes based on biomineralization process*, Mater. Sci. Eng., 2005, 25, 97–104.

[15] KULISCH W., GILLILAND D., CECCONE G., *Tantalum pentoxide as a material for biosensors: deposition, properties and applications*, [in:] *Nanostructured Materials for Advanced Technological Applications*, J. Reithmaier, P. Petkov, W. Kulisch, C. Popov (Eds.), Springer, 2009, 509–524.

[16] LI X., WANG, L., YU X., FENG Y., WANG C., YANG K., SU D., *Tantalum coating on porous Ti_6Al_4V scaffold using chemical vapor deposition and preliminary biological evaluation*, Mater. Sci. Eng. C, 2013, 33 (5), 2987–2994.

[17] MAHO A., LINDEN S., ARNOULD C., DETRICHE S., DELHALLE J., MEKHALIF Z., *Tantalum oxide/carbon nanotubes composite coatings on titanium, and their functionalization with orga-*

nophosphonic molecular films: A high quality scaffold for hydroxyapatite growth, J. Colloid Interface Sci., 2012, 371 (1), 150–158.

[18] MIYAZAKI T., KIM H.-M., KOKUBO T., *Induction and acceleration of bonelike apatite formation on tantalum oxide gel in simulated body fluid*, J. Solgel Sci. Technol., 2001, 21, 83–88.

[19] NDIEGE N., WILHOITE T., SUBRAMANIAN V., *Sol−Gel Synthesis of Thick Ta_2O_5 Films*, Chem. Mater., 2007, 19, 3155–3161.

[20] PRAMANIK S., ATAOLLAHI F., PINGGUAN-MURPHY B., OSHKOUR A.A., ABU OSMAN N.A., *In vitro study of surface modified poly (ethylene glycol)-impregnated sintered bovine bone scaffolds on human fibroblast cells*, Sci. Rep., 2015, 5, 9806.

[21] RAO K.T.V., SOUZANCHI S., YUAN Z., *One-pot sol–gel synthesis of a phosphated TiO_2 catalyst for conversion of monosaccharide, disaccharides, and polysaccharides to 5-hydroxymethylfurfural*, New J. Chem., 2019, 43, 12483–12493.

[22] SATHASIVAM S., WILLIAMSON B.A., KAFIZAS A., ALTHABAITI S.A., OBAID A.Y., BASAHEL S.N., SCANLON D.O., CARMALT C.J., PARKIN I.P., *Computational and experimental study of Ta_2O_5 thin films*, J. Phys. Chem. C, 2017, 121 (1), 202–210.

[23] SATO M., SLAMOVICH E.B., WEBSTER T.J., *Enhanced osteoblast adhesion on hydrothermally treated hydroxyapatite/titania /poly (lactide-co-glycolide) sol–gel titanium coatings*, Biomaterials, 2005, 26, 1349–1357.

[24] SHORVAZI S., KERMANI F., MOLLAZADEH S., *Coating Ti_6Al_4V substrate with the triple-layer glass-ceramic compositions using sol–gel method; the critical effect of the composition of the layers on the mechanical and in vitro biological performance*, J. Solgel Sci. Technol., 2020, 94, 743–753.

[25] SIU J.H., LI L.K., *An investigation of the effect of surface roughness and coating thickness on the friction and wear behaviour of a commercial MoS_2–metal coating on AISI 400C steel*, Wear, 2000, 237, 283–287.

[26] STOCH A., JASTRZĘBSKI W., DŁUGOŃ E., *Sol–gel derived hydroxyapatite coatings on titanium and its alloy Ti_6Al_4V*, J. Mol. Struct., 2005, 744, 633–640.

[27] SUN Y.S., CHANG J.H., HUANG H.H., *Corrosion resistance and biocompatibility of titanium surface coated with amorphous tantalum pentoxide*, Thin. Solid. Films, 2013, 528, 130–135.

[28] SUN Y.S., CHANG J.H., HUANG H.H., *Using submicroporous Ta oxide coatings deposited by a simple hydrolysis–condensation process to increase the biological responses to Ti surface*, Surf. Coat Tech., 2014, 259, 199–205.

[29] TADDEI P., TINTI A., REGGIANI M., *In vivo bioactivity of titanium and fluorinated apatite coatings for orthopaedic implants: a vibrational study*, J. Mol. Struct., 2003, 651, 427–431.

[30] TEPEHAN F.Z., GHODSI F.E., OZER N., *Optical properties of sol–gel dip-coated Ta_2O_5 films for electrochromic applications*, Sol Energy Mater. Sol Cells, 1999, 59, 265–275.

[31] TRIPATHY A., PRAMANIK S., MANNA A., AZRIN SHAH N.F., SHASMIN H.N., RADZI Z., ABU OSMAN N.A., *Synthesis and characterizations of novel Ca-Mg-Ti-Fe-oxides-based ceramic nanocrystals and flexible film of polydimethylsiloxane composite with improved mechanical and dielectric properties for sensors*, Sensors, 2016, 16, 292.

[32] WAN T., STYLIOS G.K., *Effects of coating process on the surface roughness of coated fabrics*, J. Text Inst., 2017, 108, 712–719.

[33] WOLF M.J., ROITSCH S., MAYER J., NIJMEIJER A., BOUWMEESTER H.J., *Fabrication of ultrathin films of Ta_2O_5 by a sol–gel method*, Thin Solid Films, 2013, 527, 354–357.

[34] XU J., KE BAO X., FU T., LYU Y., MUNROE P., XIE Z.H., *In vitro biocompatibility of a nanocrystalline β-Ta_2O_5 coating for orthopaedic implants*, Ceram. Int., 2018, 44 (5), 4660–4675.

[35] YU J., ZHAO X., ZHAO Q., *Effect of surface structure on photocatalytic activity of TiO_2 thin films prepared by sol-gel method*, Thin Solid Films, 2000, 379, 7–14.

[36] ZHANG P., LIN D., ZHU Y., *In-situ high temperature laser-induced damage of sol-gel Ta_2O_5 films with different dual additives*, Thin Solid Films, 2020, 693, 137723.